Intermetallics 18 (2010) 87–91

Contents lists available at ScienceDirect

Intermetallics

journal homepage: www.elsevier.com/locate/intermet

Multi-stage transformation in annealed Ni-rich $Ti_{49}Ni_{41}Cu_{10}$ shape memory alloy

Kai-Nan Lin [a], Shyi-Kaan Wu [a,b,*]

[a] Department of Materials Science and Engineering, National Taiwan University, Taipei 106, Taiwan
[b] Department of Mechanical Engineering, National Taiwan University, Taipei 106, Taiwan

ARTICLE INFO

Article history:
Received 22 August 2008
Received in revised form
13 June 2009
Accepted 16 June 2009
Available online 15 July 2009

Keywords:
A. Intermetallics, miscellaneous
B. Internal friction
B. Martensitic transformations
B. Precipitates
C. Heat treatment

ABSTRACT

Multi-stage transformation (MST) in 500 °C annealed Ni-rich $Ti_{49}Ni_{41}Cu_{10}$ shape memory alloy (SMA) is investigated by differential scanning calorimetry (DSC), dynamic mechanical analyzer (DMA), X-ray diffraction (XRD) and scanning electron microscopy (SEM). The as solution-treated alloy undergoes B2 ↔ B19 ↔ B19′ two-stage transformations. $Ti(Ni,Cu)_2$ precipitates are formed in 500 °C annealed specimens. Alloy annealed at 500 °C for 6–24 h exhibits MST. This MST is confirmed by DMA tests and is composed of $B2_1$ ↔ $B19_1$ ↔ $B19'_1$ and $B2_2$ ↔ $B19_2$ ↔ $B19'_2$ transformations corresponding to the regions near and far from $Ti(Ni,Cu)_2$ precipitates, respectively. Experimental results show that the more the annealing time, the more the $B2_1$ ↔ $B19_1$ ↔ $B19'_1$ transformations and finally only $B2_1$ ↔ $B19_1$ ↔ $B19'_1$ transformations retain with the transformation temperatures close to those of $Ti_{50}Ni_{40}Cu_{10}$ SMA.

1. Introduction

TiNi-based shape memory alloys (SMAs) are known as having high potential for industrial and biomedical applications owing to their excellent properties on shape memory effect (SME), pseudoelasticity (PE) and damping capacity (DC) [1]. Among ternary TiNi-based SMAs, $Ti_{50}Ni_{50-x}Cu_x$ SMAs with $x < 30$ at.% have been investigated extensively from various aspects, such as SME [2–4], martensitic transformation behaviors [5], mechanical characteristics, microstructures [6–8], internal friction [9–13], etc. The substitution of Cu for Ni in TiNi SMAs has been known to reduce the composition sensitivity for M_s, the starting temperature of martensitic transformation, and to prevent the precipitation of Ti_3Ni_4 precipitates.

Multi-stage transformation (MST) has been widely investigated in TiNi-based SMAs. Bataillard et al. [14] and Khalil-Allafi et al. [15] reported that the MST in annealed Ni-rich TiNi SMAs is associated with the stress field and the heterogeneous Ni content caused by Ti_3Ni_4 precipitates which is called small-scale heterogeneity. Khalil-Allafi et al. [16,17] and Fan et al. [18] further reported that the MST is resulted from the inhomogeneous distribution of Ti_3Ni_4 precipitates in annealed Ni-rich TiNi SMAs, i.e. Ti_3Ni_4 precipitates are abundant near grain boundaries and free in grain interior which is called large-scale heterogeneity. In order to eliminate the grain boundary effect and to identify the effect of small-scale heterogeneity on the MST, Eggeler et al. [19] investigated the MST in Ni-rich TiNi single crystals with homogeneously distributed Ti_3Ni_4 precipitates. They concluded that the MST appears when the interparticle spacing of Ti_3Ni_4 precipitates reaches a critical value of about 200 nm. In addition to Ti_3Ni_4 precipitates in annealed Ni-rich TiNi SMAs, the MST also appears due to the occurrence of different grain-size distribution in cold-rolled and annealed $Ti_{50}Ni_{50}$ SMA [20], in annealed melt-spun $Ti_{51}Ni_{49}$ SMA ribbons [21] and in cold-rolled and annealed Ti-rich $Ti_{51}Ni_{40}Cu_9$ SMA [22].

However, up to now, few studies have been reported on the MST of annealed Ni-rich TiNiCu SMAs. Fukuda et al. [23] reported that, by differential scanning calorimetry (DSC), electrical resistivity and transmission electron microscope (TEM) tests, the plate-like $Ti(Ni,Cu)_2$ precipitates in 600 °C annealed $Ti_{49.5}Ni_{40.5}Cu_{10}$ SMA can separate B2 ↔ B19 transformation from one transformation peak into two transformation peaks. But this report did not well describe the effect of $Ti(Ni,Cu)_2$ precipitates on B19 → B19′ transformation. In the present study, we investigate the MST in annealed Ni-rich $Ti_{49}Ni_{41}Cu_{10}$ SMA by DSC, dynamic mechanical analyzer (DMA), X-ray diffraction (XRD) and scanning electron microscopy (SEM). The MST induced by $Ti(Ni,Cu)_2$ precipitates in 500 °C annealed $Ti_{49}Ni_{41}Cu_{10}$ SMA is found and the transformation sequence of the MST is discussed.

* Corresponding author. Department of Materials Science and Engineering, National Taiwan University, Taipei 106, Taiwan. Tel.: +886 2 3366 4483; fax: +886 2 2363 4562.
E-mail address: skw@ntu.edu.tw (S.-K. Wu).

0966-9795/$ – see front matter © 2009 Elsevier Ltd. All rights reserved.
doi:10.1016/j.intermet.2009.06.011

2. Experimental procedures

$Ti_{49}Ni_{41}Cu_{10}$ (in at.%) ingot was prepared by vacuum arc-remelter (VAR) in which high purity Ti (99.7 wt.%), Ni (99.9 wt.%) and Cu (99.99 wt.%) were remelted six times in a high purity Ar atmosphere. The as-melted ingot was hot-rolled at 900 °C to a plate of 1.8 mm thickness by STANAT TA-515-5-5X8 rolling machine at a constant rolling speed of 10 m/min. Thereafter the plate was solution-treated at 900 °C for 1 h and then water-quenched. The oxidation layer of the plate was chemical etched by a solution composed of $HF:HNO_3:H_2O = 1:5:20$ (in volume) and then polished by #150 sandpaper. After removing the oxidation layer, the plate was cut into 45 mm × 6.5 mm × 1.6 mm specimens with the longitude along the hot-rolling direction. These specimens were then sealed in evacuated quartz tubes and annealed at 500 °C for different time intervals, and subsequently quenched into water. Transformation peak temperatures and transformation enthalpy were determined by TA Q10 DSC equipment with 10 °C/min cooling/heating rate and the weight of DSC specimens was about 30 mg. The DMA tests were conducted by TA 2980 DMA equipment with 3 °C/min cooling rate under constant frequency (1 Hz) and amplitude (5 μm) of single cantilever mode. The size of DMA specimens was about 35 mm × 6.5 mm × 1.5 mm. The testing temperature range was taken from +150 °C to −150 °C for DSC tests and from +150 °C to −120 °C for DMA tests. The isothermal DMA test was conducted under the same cooling rate, frequency and amplitude mentioned above and followed the sequence: (1) held at 150 °C for 1 min, (2) cooling down to peak temperature and (3) held at peak temperature for 30 min. XRD tests were conducted by PANalytical PW3040 instrument equipped with Cu Kα radiation at room temperature. The applied voltage, applied current, scanning range and step size were set at 45 kV, 40 mA, 30°–50° and 0.02°/step, respectively. The specimens for XRD tests were cut and ground to about the size of 12 mm × 6.5 mm × 1.5 mm and then polished by #2000 sandpaper. Before XRD tests, the specimens were cooled down in liquid nitrogen and then heated up to room temperature (25 °C). SEM tests were conducted by LEO-1530 field emission SEM. The specimens for SEM tests were polished by 0.5 μm Al_2O_3 and then etched by a solution composed of $HF:HNO_3:H_2O = 4:5:20$ (in volume) for 3–5 sec.

3. Results and discussion

3.1. Transformation sequence of as solution-treated $Ti_{49}Ni_{41}Cu_{10}$ alloy

Fig. 1(a)–(c) shows DSC curves, DMA curves and isothermal DMA results, respectively, of as solution-treated $Ti_{49}Ni_{41}Cu_{10}$ SMA. From Fig. 1(a), a typical two-stage B2 ↔ B19 ↔ B19′ transformation is observed. The peak temperatures of B2 → B19 and B19 → B19′ transformations in cooling curve, and those of B19′ → B19 and B19 → B2 transformations in heating curve are −38.2 °C, −112.9 °C, −93.1 °C and −22.2 °C, respectively. Transformation enthalpies during cooling and heating are 12.3 J/g and 12.5 J/g, respectively. The results of transformation temperatures and enthalpies shown in Fig. 1(a) are all lower than those of $Ti_{50}Ni_{40}Cu_{10}$ SMA [9]. This decrease can be explained by the Ni-rich content in $Ti_{49}Ni_{41}Cu_{10}$ SMA. At the same time, B19 ↔ B19′ transformation peaks shown in Fig. 1(a) are quite broad and small and their peak temperatures are not easy to measure accurately.

In our previous study [13], DMA has been confirmed to be more suitable than DSC for investigating the transformation behavior of $Ti_{50}Ni_{40}Cu_{10}$ SMA because DMA test can exhibit significant tan δ peaks and deep storage modulus (E_0) minima for both B2 → B19 and B19 → B19′ transformations. Thus, DMA test was further conducted on as solution-treated $Ti_{49}Ni_{41}Cu_{10}$ SMA to reveal the existence of B19 → B19′ transformation, as shown in Fig. 1(b). From Fig. 1(b), two tan δ peaks and their corresponding E_0 minima of B2 → B19 and B19 → B19′ transformations are indicated by arrows. Moreover, isothermal DMA test was also conducted to confirm these two peaks to be transformation peaks, as shown in Fig. 1(c). In our previous study [12], the isothermal drops of B2 → B19 and B19 → B19′ transformation tan δ peaks in $Ti_{51}Ni_{39}Cu_{10}$ SMA are measured to be 81.9% and 81.2%, respectively, when the specimen was kept isothermal at transformation peak temperatures for 30 min. From Fig. 1(c), the isothermal drops of B2 → B19 and B19 → B19′ peaks are 78.4% and 79.8%, respectively. It reveals that the isothermal drops of these two tan δ peaks are quite similar to

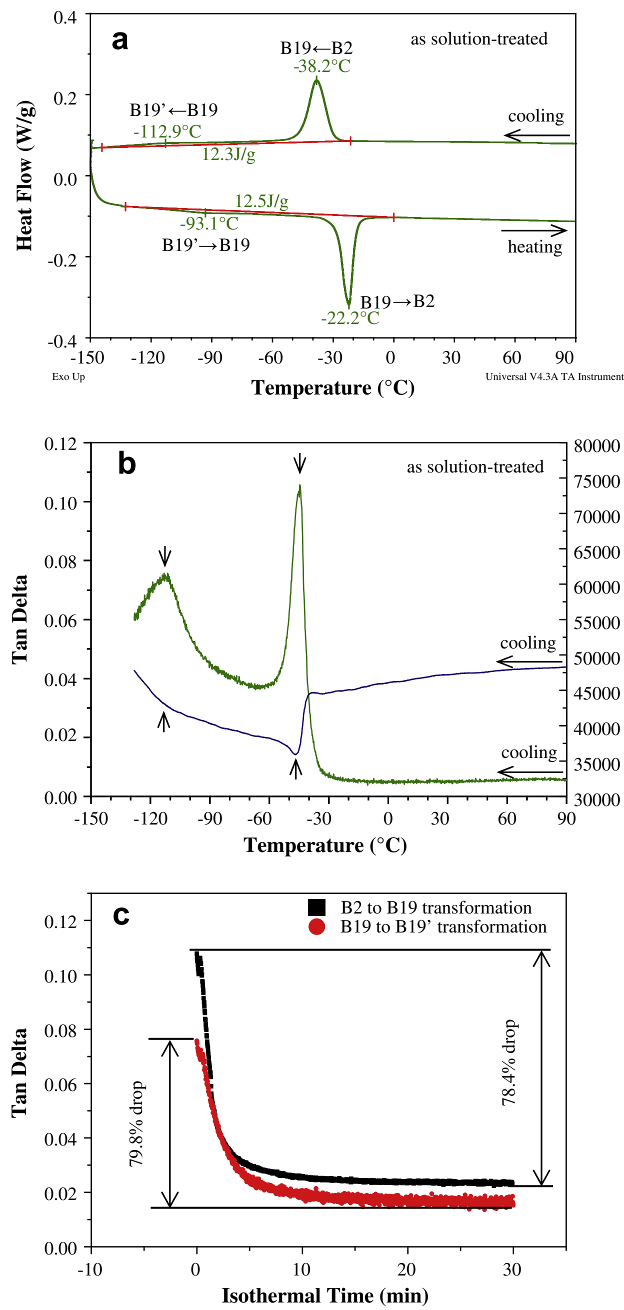

Fig. 1. (a) DSC curves, (b) DMA curves and (c) DMA isothermal results of solution-treated $Ti_{49}Ni_{41}Cu_{10}$ SMA.